PROCEEDINGS OF SCIENCE

Higgs boson differential and STXS measurements - bosonic channels

Alessandro Tarabini[a,*] **on behalf of the CMS collaboration**

[a] *Laboratoire Leprince-Ringuet, CNRS/IN2P3, Ecole Polytechnique, Institut Polytechnique de Paris, Palaiseau, France,*
Route de Saclay, 91128 PALAISEAU CEDEX

E-mail: alessandro.tarabini@cern.ch

This proceeding covers fiducial Higgs boson cross section measurements and simplified template cross section measurements by the CMS collaboration. The report focuses on measurements in bosonic decay channels, namely $H \to \gamma\gamma$, $H \to ZZ \to 4\ell$, and $H \to WW \to 2\ell 2\nu$, and all measurements are performed using Run 2 data (2016-2018) at a centre of mass energy of 13 TeV. All results are found to be in agreement with the Standard Model of particle physics.

41st International Conference on High Energy physics - ICHEP2022
6-13 July, 2022
Bologna, Italy

*Speaker

PoS(ICHEP2022)509

1. Introduction

The Compact Muon Solenoid (CMS) experiment [1] is one of the two multi-purpose experiments at the CERN LHC. Since the discovery of the Higgs boson [2, 3, 5], the measurements of its cross sections have been used as a key tool to nail down the Higgs boson properties. This note presents the CMS Run 2 results of the bosonic decay channels of the Higgs boson ($H \to \gamma\gamma$, $H \to ZZ \to 4\ell$, $H \to WW \to 2\ell 2\nu$).

2. Simplified Template Cross Sections

Simplified Template Cross Sections (STXS) have been adopted as a common framework by the LHC experiments for Higgs boson measurements. The STXS scheme is centrally provided by the LHC Higgs Working Group and it is designed to maximise the sensitivity to effects from Beyond-Standard-Model (BSM) physics while reducing theory dependence. Then, each analysis, depending on its sensitivity and features, merges some STXS bins to avoid large uncertainties or high correlations between measured parameters. However, merging bins reduces the model-independence, hence a trade-off is usually found. All results presented here are based on the stage 1.2 of the STXS framework, which is an improvement developed from the first partial Run 2 results of the previous stage 1.1 [4].

2.1 $H \to \gamma\gamma$

In the $H \to \gamma\gamma$ analysis [6] there is an extensive use of Boosted Decision Trees (BDTs) and Deep Neural Networks (DNNs) to build categories targeting STXS bins. Two sets of results with two levels of granularity are presented:

- **Maximal merging scenario *(Figure 1a)*** The rule of thumb is to combine STXS bins together until the expected uncertainty in the cross section measurement is less than 150% of the Standard Model (SM) prediction. To be noted, the ggH BSM bin (with $p_T^H > 200$ GeV), which is sensitive to BSM physics entering the ggH loop, is measured with an uncertainty lower than 40% and it is consistent with the SM prediction. Another result to be highlighted is the tH production mode that is measured separately from ttH (usually in the stage 1.2 they are measured together) and this is the best tH measurement up to date with an observed (expected) limit at 95% of CL equal to 14 (8) times the SM value.
- **Minimal merging scenario *(Figure 1b)*** Only few bins are merged together whilst ensuring that parameters do not become too anti-correlated (less than 90%). For instance, VBF-like bins in ggH and qqH are measured together to avoid large correlations. A result to be mentioned is the differential measurement of ttH production in p_T^H, it is the only channel providing such a measurement.

2.2 $H \to ZZ \to 4\ell$

One of the characteristics of the STXS measurements in the $H \to ZZ \to 4\ell$ channel [7] is the extensive use of kinematic discriminants based on matrix-element probabilities. They are used in the event selection, to build STXS categories, and in the 2D likelihood fit.

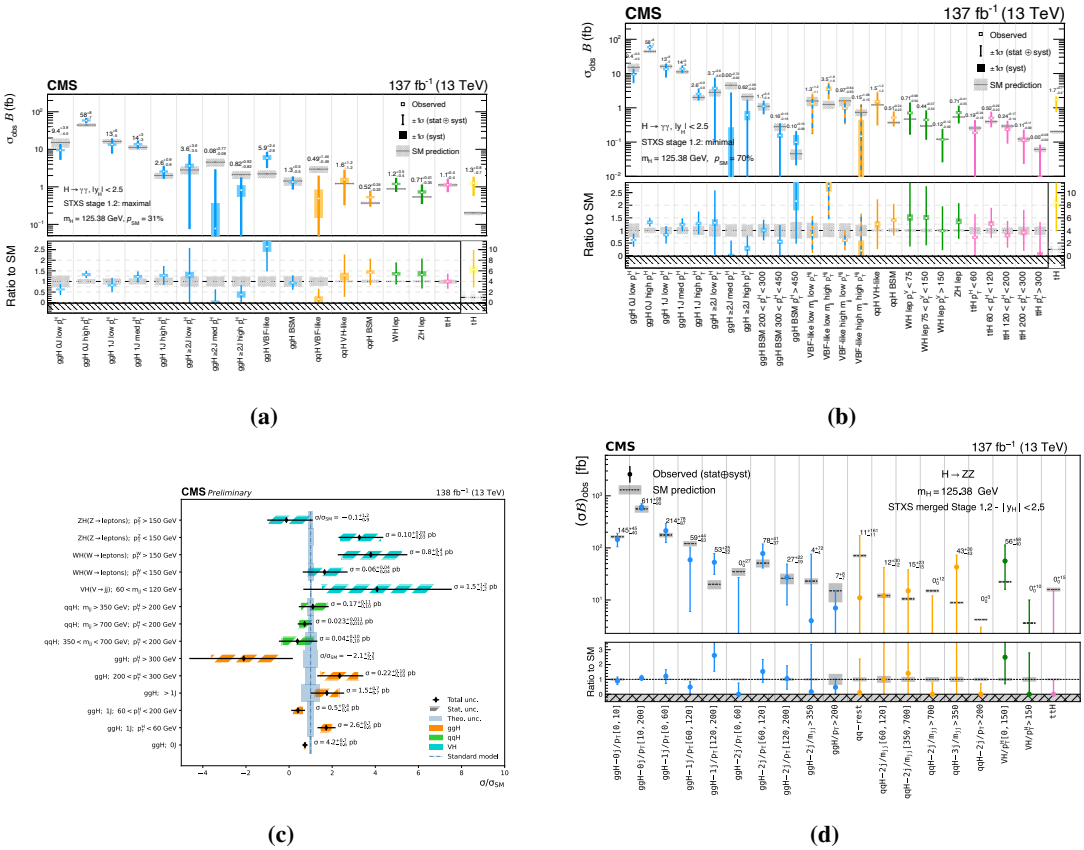

Figure 1: STXS results. (a) Minimal merging scenario in $H \to \gamma\gamma$ [6]. (b) Maximal merging scenario in $H \to \gamma\gamma$ [6]. (c) Results in $H \to WW$ [8]. (d) Results in $H \to ZZ \to 4\ell$ [7].

Here, because of the low number of events, many bins have been merged and the best-fit cross section in some of these bins, such as ttH and the high-m_{jj} VBF bin, is found to be 0. On the other hand, the cross sections in some of the ggH bins are measured with a precision of up to 16%. The results are reported in Fig. 1d.

2.3 $H \to WW \to 2\ell 2\nu$

In the STXS analysis of the $H \to WW \to 2\ell 2\nu$ decay channel [8] both opposite-flavour $H \to WW \to e^{\pm}\mu^{\mp}\nu\bar{\nu}$ and same-flavour $H \to WW \to e^{+}e^{-}(\mu^{+}\mu^{-})\nu\bar{\nu}$ final states are considered. Like in the $H \to \gamma\gamma$ measurement, DNNs are used to build categories. This analysis targets only the ggH, qqH, and VH production modes, and a good sensitivity is attained for ggH, especially at low-pT. The results are reported in Fig. 1c.

3. Fiducial Cross Sections

Inclusive and differential fiducial cross sections have been widely used since Run 1 and they are optimised for maximal theory independence. Thanks to the large data set collected during Run 2, the number of fiducial observables is growing and so is the number of bins that can be probed

in these observables. Concerning the choice of bin boundaries, an important step in each fiducial analysis, they are chosen following three criteria: bin alignment to ease combination, ensuring a sufficient number of events to have a low expected uncertainty on the cross section, and a good level of signal-to-background ratio.

3.1 $H \to \gamma\gamma$

The $H \to \gamma\gamma$ fiducial analysis [9] provides a wide range of both inclusive and differential measurements to fully characterise the decay channel. The inclusive cross section is measured in dedicated phase-space regions designed to loosely target specific production modes. The inclusive measurement in a VBF-enriched phase-space is also provided and several jet-related differential observables are measured in this region, as well. To inspect the phase-space further, some double-differential observables are measured (Fig. 2b).

A rapidity-weighed jet observable [10] (Fig. 2a) is measured for the first time. Binning in such observables rather than in p_T^{jet} does not introduce extra logarithms (or minimises their contribution) in the resummation region (low-pT) of the ggH cross section computation, leading to precise theoretical results and a test of QCD resummation.

The inclusive cross section is measured to be:

$$\sigma_{fid} = 73.4^{+6.1(8.3\%)}_{-5.9(8.0\%)} \text{ fb} = 73.4^{+5.4(7.4\%)}_{-5.3(7.2\%)} \text{ (stat.)}^{+2.4(3.3\%)}_{-2.2(3.0\%)} \text{ (sys.) fb}$$

to be compared with the SM expectation of $75.4 \pm 4.1(5.4\%)$. The precision of the measured value is very close to the expected's, and the systematic component is well below the theoretical precision.

3.2 $H \to ZZ \to 4\ell$

The four-lepton fiducial analysis [7] quotes the integrated cross section in the three possible final states ($\sigma_{2e2\mu} = 1.31^{+0.20}_{-0.19}$ fb, $\sigma_{4\mu} = 0.78^{+0.10}_{-0.10}$ fb, $\sigma_{4e} = 0.76^{+0.18}_{-0.16}$ fb) and in the inclusive one:

$$\sigma_{fid} = 2.84^{+0.34(12.0\%)}_{-0.31(10.9\%)} \text{ fb} = 2.84^{+0.23(8.1\%)}_{-0.22(7.7\%)} \text{ (stat.)}^{+0.26(9.2\%)}_{-0.21(7.4\%)} \text{ (sys.) fb}$$

to be compared with the SM expectation of $2.84 \pm 0.15(5.3\%)$. The systematic and statistical component contribute similarly to the final uncertainty.

The differential distribution in transverse momentum of the Higgs is reported in Fig. 2c. All results are extracted by floating the branching ratio of the Higgs boson in four leptons to increase the model independence and to be sensitive to possible BSM effects in the decay.

3.3 $H \to WW \to 2\ell 2\nu$

Unlike the corresponding STXS analysis, in the fiducial analysis [11] only the opposite-flavour $H \to WW \to e^{\pm}\mu^{\mp}\nu\bar{\nu}$ final state is considered to suppress the Drell-Yan background. The measured fiducial signal strength is measured to be:

$$\mu_{fid} = 1.05 \pm 0.12(11.4\%) = 1.05 \pm 0.05\ (4.8\%)(\text{stat.}) \pm 0.10\ (9.5\%)(\text{sys.})$$

and the corresponding SM fiducial cross section is $82.5 \pm 4.2(5.1\%)$fb. In this decay channel the systematic component leads the uncertainty whereas the statistical counterpart, thanks to the large branching ratio, is the smallest among the bosonic decay channels.

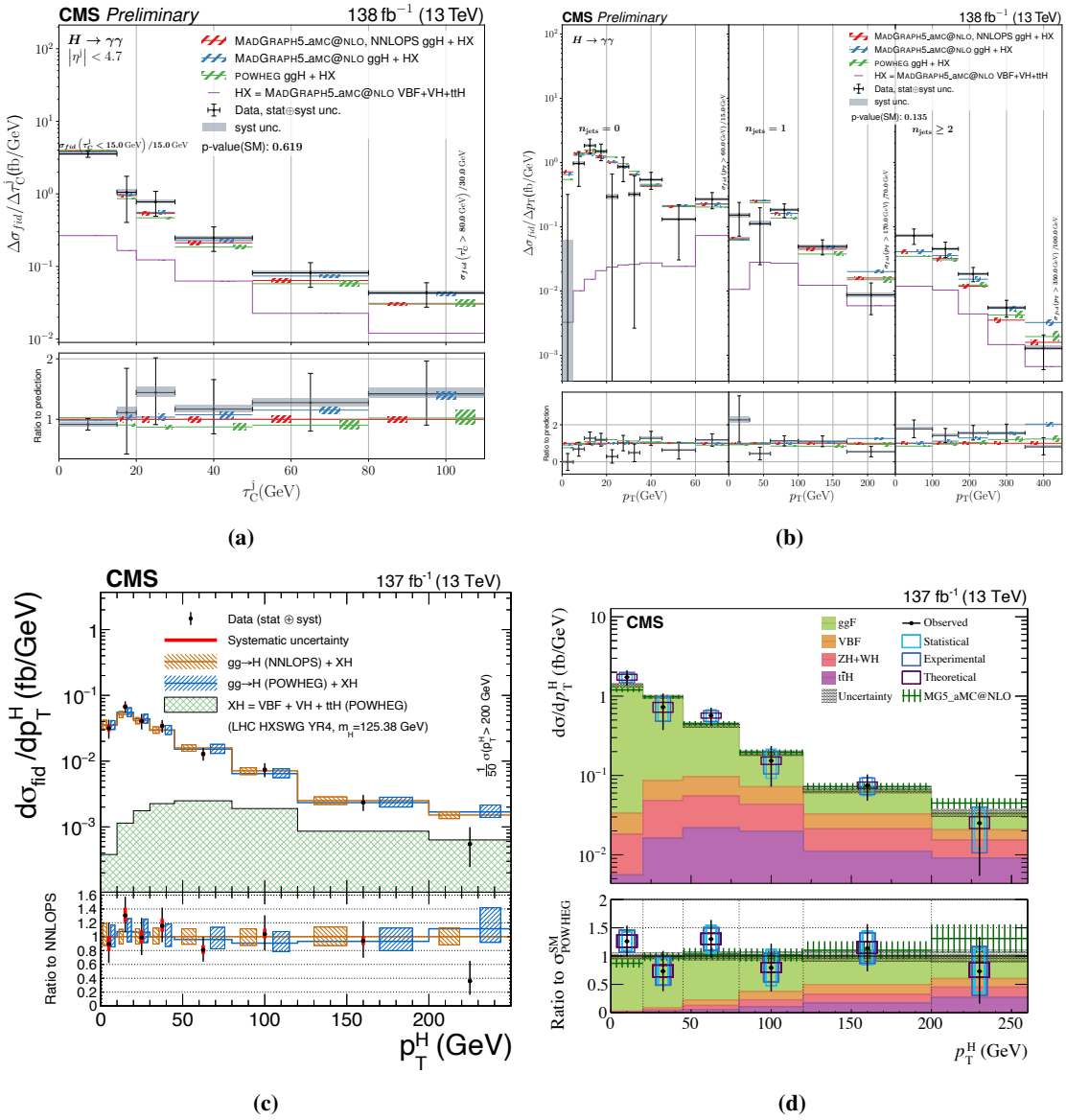

Figure 2: Differential fiducial measurements. (a) Rapidity-weighed jet observable in $H \to \gamma\gamma$ [9]. (b) Double-differential observable p_T^H vs N_{jet} in $H \to \gamma\gamma$ [9]. (c) Fiducial cross sections in bins of transverse momentum of the Higgs boson in $H \to ZZ \to 4\ell$ [7]. (d) Fiducial cross sections in bins of transverse momentum of the Higgs boson in $H \to WW \to 2\ell 2\nu$ [11].

Two differential observables are measured: the number of associated jets and the transverse momentum of the Higgs boson. The p_T^H binning is coarser with respect to the other channels presented in this proceeding. One of the requirements when setting the bin boundaries is to ensure a larger bin width than the p_T^H resolution. In the $H \to WW$ channel the momentum resolution is dominated by the resolution on the missing transverse momentum (~20 GeV), and at high-p_T the binning is even coarser to avoid expected uncertainty over 100%. Additionally, the unfolding matrix of this variable has large off-diagonal elements, hence a regularised unfolding is implemented to extract the cross section. The distribution is reported in Fig. 2d.

4. Conclusion

Fiducial cross sections and STXS provide two complementary ways to measure the Higgs boson properties and this note presents the CMS Run 2 results in the bosonic decay channels. All results show an overall good agreement with the SM and no significant deviations have been found. The precision of the inclusive results is around 10% and is getting close to the precision of theoretical predictions, similarly the differential results are becoming finer and finer as we increase the size of the data set. We are officially entering in the precision era for Higgs boson physics, where the properties of the scalar sector will be investigated with high precision and granularity.

References

[1] CMS Collaboration, "The CMS experiment at the CERN LHC", JINST 3 S08004 (2008)

[2] CMS Collaboration, "Observation of a new boson at a mass of 125 GeV with the CMS experiment at the LHC", *Phys.Lett.* **B716** (2012) 30-61, doi:10.1016/j.physletb.2012.02.021, arXiv:1207.7235

[3] ATLAS Collaboration, "Observation of a new particle in the search for the Standard Model Higgs boson with the ATLAS detector at the LHC", *Phys.Lett.* **B716** (2012) 1-29, doi:10.1016/j.physletb.2012.08.020, arXiv:1207.7214

[4] Berger, Nicolas et al., "Simplified Template Cross Sections - Stage 1.1", arXiv:1906.02754

[5] CMS Collaboration, "Observation of a new boson with mass near 125 GeV in pp collisions at $\sqrt{s}$ = 7 and 8 TeV", *JHEP* **06** (2013), 081, doi:10.1007/JHEP06(2013)081, arXiv:1303.4571.

[6] CMS Collaboration, JHEP **07** (2021), 027 doi:10.1007/JHEP07(2021)027 [arXiv:2103.06956 [hep-ex]].

[7] CMS Collaboration, Eur. Phys. J. C **81** (2021) no.6, 488 doi:10.1140/epjc/s10052-021-09200-x [arXiv:2103.04956 [hep-ex]].

[8] CMS Collaboration, CMS-PAS-HIG-20-013, https://cds.cern.ch/record/2803738.

[9] CMS Collaboration, CMS-PAS-HIG-19-016, https://cds.cern.ch/record/2803740.

[10] CMS Collaboration, Phys. Rev. D **91** (2015) no.5, 054023 doi:10.1103/PhysRevD.91.054023 [arXiv:1412.4792 [hep-ph]].

[11] CMS Collaboration, JHEP **03** (2021), 003 doi:10.1007/JHEP03(2021)003 [arXiv:2007.01984 [hep-ex]].

PoS(ICHEP2022)509